Solid State Science and Technology, Vol. 28, No 1 & 2 (2020) 87-102
ISSN 0128-7389 | *http://myjms.mohe.gov.my/index.php/masshp*

ELECTROSPUN NANO-PALM FROND TITANIA FIBER (NANO-PFTF) MEMBRANE FOR INDUSTRIAL WASTEWATER TREATMENT

Ismail I. N. Ismail[1,*], R. A. Zayadi[2], K. C. Ho[3], J. Z. Soo[4], M. S. Idris[5], K. Y. Tay[6], N. A. Kamaruzaman[1]

[1]*National Nanotechnology Centre (NNC), Ministry of Science, Technology and Innovation (MOSTI), 62662 Putrajaya, Malaysia*

[2]*Department of Physics and Chemistry, Universiti Tun Hussein Onn Malaysia (UTHM), Pagoh Edu Hub, 84600 Johor, Malaysia*

[3]*Centre of Water Research, Faculty of Engineering, Built Environment, and Information Technology, SEGi University, Jalan Teknologi, Kota Damansara, 47810 Petaling Jaya, Selangor, Malaysia*

[4]*Department of Electronic Materials Engineering, Research School of Physics, The Australian National University, Canberra, Australian Capital Territory 2601, Australia*

[5]*Boston Scientific Medical Device (Malaysia) Sdn. Bhd., PMT 741, Persiaran Cassia Selatan 1, Lebuhraya Bandar Cassia, Taman Perindustrian Batu Kawan, 14110 Penang, Malaysia*

[6]*Hi-Tech Instruments Sdn. Bhd., 19, Jalan BP 4/8, 47120 Bandar Bukit Puchong, Selangor, Malaysia*

[*]*Corresponding author:* ismarul@mosti.gov.my

ABSTRACT

In this project, Nano-Palm Frond Titania Fiber (Nano-PFTF) membrane was fabricated using cellulose acetate (CA) derived from oil palm frond (OPF). The nanofiber membrane combines adsorption and photocatalytic degradation of the pollutants by nitrogen-doped titanium dioxide (N-TiO_2). The synthesized CA, N-TiO_2, and Nano-PFTF membrane were characterized using Raman spectroscopy and field emission scanning electron microscope (FESEM). The efficiency of the fabricated Nano-PFTF membrane was tested with methylene blue (MB) dye and hexavalent chromium (Cr (VI)) under UV-C and visible light irradiation. Within 120 minutes, 97.82 % rejection percentage of 10 ppm MB was achieved by Nano-PFTF membrane (CA/N-TiO_2) while 99 % rejection percentage of 10 ppm Cr (VI) was achieved by Nano-PFTF membrane under visible and UV light irradiation respectively. Based on the results, the Nano-PFTF membrane showed remarkable potential in industrial wastewater treatment and increase the potential usefulness of OPF.

INTRODUCTION

Increasing world's population increases the occurrence of water pollution due to anthropogenic activities. The introduction of organic pollutants such as textile dye and heavy metals in water bodies due to industrial activities creates an alarming need for efficient pollutants removal from wastewater. This is because these pollutants can pose detrimental effects towards aquatic and human health when left untreated. Each year, over 700,000 tons of dyes are used in textile industry with 2-20% are directly discharged into wastewater as aqueous effluent [1]. Textile dyeing is considered as the main contributor of water pollution where about 200 billion liters of colored effluents need to be treated annually [2]. There are about 3,600 to 10,000 commercial synthetic dyes available; each with different fixation rate [2,3]. Up to 50% of the dyes used in the dyeing process are not fixed to the fiber thus enter the drains and potentially harm the environmental health with the release of persistent organic pollutants [1,4]. On the other hand, heavy metals can be both naturally occurring and from anthropogenic activities; commonly associated with industries like electronic, textile, mining, and electroplating. Among the heavy metals that are of public health interest due to their toxicity are arsenic, cadmium, chromium, lead, and mercury [5,6].

Titanium dioxide (TiO_2) or titania is a semiconductor metal oxide that is widely used as a photocatalyst in wastewater pollutant degradation. TiO_2 can be activated by UV photon energy to produce highly reactive radicals to degrade organic contaminants. TiO_2 is highly favored because of its high stability and photocatalytic performance, non-toxicity, and biocompatibility [11,12]. Previous studies had shown that TiO_2 has remarkable potential in degrading organic and inorganic pollutants such as dyes and heavy metals [11,13,14]. However, intrinsic TiO_2 has large energy bandgap (E_{BG}) at 3.0 eV (415 nm) for rutile TiO_2 and 3.2 eV (380 nm) for anatase TiO_2), in which only UV light can be used to activate it [15–17]. Doping TiO_2 with non-metal impurities such as nitrogen (N-TiO_2) helps to shift the E_{BG} of TiO_2 into the visible light region [13,14]. This allows TiO_2 to utilize broader spectrum of the solar irradiation which is composed of about 4-5% of UV light and 40% of visible light [12,17]. In addition, incorporating TiO_2 in nanostructure supports such as nanofibers help to reduce potential TiO_2 particle agglomeration, ensuring a consistently higher pollutant degradation performance.

At the same time, Malaysia is reputed as one of the world's largest producers and exporters of palm oil. . The total production of palm oil biomass reached 90 million tons in 2017, with more than half contributed by oil palm fronds (OPF) [7]. To improve the sustainability of manufacturing palm oil, it is imperative to reduce the high levels of palm oil biomass has intensified, among which is to reuse oil palm biomass including the OPF or other purposes. One particular area of interest is to extract cellulose and cellulose-based derivatives from OPF, given its large cellulose composition (39.4-47.3%). [8]. Notably, cellulose acetate (CA) is commonly used as a natural polymer component for nanofiber membrane due to its high surface area, low density, and high mechanical performance [9,10]. As nanofibers are commonly derived from petroleum-based polymers such as PVP and PVA, utilizing natural-based CA from the abundantly

sourced OPF provides significant benefits both in terms of cost and environmental aspects.

In this study, we are proposing Nano-Palm Frond Titania Fiber (Nano-PFTF) membrane as a solution towards treating organic and inorganic pollutants in industrial wastewater via adsorption and photocatalytic pollutant degradation. This material combines both visible-light active N-TiO_2 nanoparticles suspended on electrospun OPF-derived CA nanofibers. . To assess the performance of this membrane, it is tested on organic textile dye; methylene blue (MB), and heavy metal pollutant; hexavalent chromium (Cr (VI)). The immobilization of N-TiO_2 in the CA nanofiber membrane in our reported study allows for easier recovery of nanomaterials after the photocatalytic degradation process. Besides, it is hypothesized the hybrid between adsorption by CA nanofiber membrane and photocatalysis by TiO_2 has synergistic effect on the removal of organics and heavy metal.

EXPERIMENTAL DETAILS

Extraction of cellulose from OPF

Cellulose was extracted from OPF using the modified method reported by Rasli et al., [10]. An amount of 50 g dried OPF was treated with 600 ml of 4% sodium hydroxide (NaOH) at 70-80°C for 3 h with constant stirring. Then, a bleaching treatment was done using 600 ml hydrogen peroxide (H_2O_2) at 70-80^{o}C for 4 h with continuous stirring. The alkali and bleaching treatments were repeated two times, respectively. After each treatment, the samples were rinsed using distilled water. The extracted cellulose was dried in an oven at 60 °C.

Acetylation and characterization of OPF-cellulose

Extracted cellulose was then undergone acetylation to produce CA [18]. 10 g of cellulose was first reacted with 110 ml of glacial acetic acid at 37.8°C for 1 h with continuous stirring. After that, the product was reacted with mixture of 40 ml of glacial acid and 0.1 ml of sulfuric acid (H_2SO_4) for 45 min with continuous stirring. The mixture was then cooled to 18.3°C before subjected to mixture of 30 ml of acetic anhydride and 0.6 ml of H_2SO_4 at 35°C for 1.5 h. Subsequently, a mixture of 10 ml of water and 20 ml of glacial acetic was added dropwise into the resulted mixture and stirred for 1 h. Lastly, the CA washed with distilled water till pH 7 before dried in oven at 60°C. The chemical bonds of CA were verified using Raman spectroscopy (Horiba, LabRam HR Evolution).

Synthesis and characterization of N-TiO_2

N-TiO_2 was synthesized based on the sol-gel method by Dhanya and Sugunan [19]. In this method, titanium isopropoxide (TTIP) and urea were taken in the mole ratio 1:5. The urea solution was added dropwise to a mixture of TTIP and ethanol. After stirring for 24 h at room temperature, it was dried at 60°C. Prior to characterization, all the samples were calcined in air using furnace (Protherm PLF 100/6) at 300°C for 4 h. The morphology and particles size of nanoparticle were observed using FESEM (JEOL

JSM-7600F and Hitachi SU8230). The purity, chemical bonding, and crystallinity of the N-TiO_2 were studied by Raman spectroscopic analyses (Horiba LabRam HR Evolution).

Synthesis and characterization of Nano-PFTF membrane

The polymer solution for electrospinning of Nano-PFTF membrane was produced by dissolving 14.5 wt. % CA in 4.22 ml of N-N-dimethyl acetamide (DMAc) and 10 ml of acetone with constant stirring at room temperature for 2 h. Then, 2 wt. % of N-TiO_2 was added slowly into the mixture, followed by 2 h of magnetic stirring. After that, the mixture was sonicated for 4 h at room temperature. Pure CA and 2 wt. % TiO_2 solution were also prepared at the same method as a control. The formulations of the synthesized membrane are summarized in Table 1.

Table 1: Electrospun membrane formulation

Membrane nomenclature	CA (wt.%)	Ratio of solvent DMAC	Acetone	Nanomaterial (wt.%)
M1	14.5	1	2	-
M2				2 wt.% TiO_2
M3				2 wt.% N-TiO_2

Electrospinning was done by loading 10 ml of the homogeneous solution to a plastic syringe attached to a stainless steel 18-gauge needle. The needle was connected using alligator clips to a high voltage power supply (Gamma High Voltage, ES30P-5W) that can provide up to 35kV. The polymeric solution is injected at a rate of 0.5 ml/h with the aid of a syringe pump (Terumo Terufusion TE-331). An aluminum foil covered on a custom-made rotating drum at the tip to collector distance of 10 cm with the rotating speed of 105 rpm serves as the collector to retrieve the deposited fibers. When a voltage was applied, the solution was charged and ejected. The solution jet travelled in the air with the evaporation of the solvent. Eventually, the fibers were collected on the grounded collector as a membrane. The fabricated membranes were characterized using scanning electron microscopy (SEM, Phenom Pro) and FESEM (JEOL, JSM-7500F) at an accelerating voltage of 10kV to obtain the fiber morphology. Chemical bonding and crystallinity of the synthesized membranes were studied by Raman spectroscopic analyses (Renishaw inVia).

Preparation of MB dye and Cr (VI)

MB was purchased from Across Chemicals and used without further modification. The absorbance of MB was measured using a UV-VIS spectrophotometer (HACH DR1900) at wavelength 660 nm. Stock solution (1000 mg/L) of Cr (VI) was prepared by dissolving potassium dichromate ($K_2Cr_2O_7$) into distilled water. The pH of the solution was adjusted to pH 2-3 using hydrochloric acid (HCl). The Cr (VI) concentrations were measured using diphenylcarbarzide (BDH) colorimetric method with a UV-VIS spectrophotometer (HACH DR1900) at wavelength 540 nm according to standard methods for the examination of water and wastewater.

Photocatalytic reduction of MB dye and Cr (VI)

The photocatalytic capabilities of the Nano-PFTF membranes in reducing MB dye and Cr (VI) are tested in batch photodegradation experiment. The membranes (0.1 g and 1 g) were placed in a quartz cell with working volume of 50 ml. The 10 ppm MB dye solution in the reactor was constantly stirred via a magnetic stirrer. All experiments were carried out within 2 h as reaction time. At 15 mins time intervals, certain volume of solution was taken and measured for the concentration. To ensure uniformity of working volume, the taken solution is refilled back into the quartz cell after concentration measurement. For control experiment, the experiment was conducted by covering the quartz cell with aluminium foil. Whereas, for UV and visible light experiment, the experiments were conducted under a light source of a 95 W UVC lamp and a 125 W visible light lamp, respectively. The optimized sets of membrane were repeated for 10 ppm of Cr (VI) to evaluate its performance in removal of heavy metal.

RESULTS AND DISCUSSION

Synthesis of CA from OPF

The synthesized CA from OPF was characterized using Raman spectroscopy with near-infrared laser (785 nm) and Raman spectra was plotted in Figure 1. Characteristic Raman signals for cellulose are observed at 1121 cm^{-1} and 2934 cm^{-1} representing asymmetric stretching vibration of C-O-C and C-H stretching respectively. Acetyl group is also present in the CA with the Raman signals noted at 1382 cm^{-1} (symmetric vibration of C-H), 1435 cm^{-1} (asymmetric vibration of C-H) and 1736 cm^{-1} (vibration of C=O) corresponding to the Raman spectrum of CA as outlined by Sánchez-Márquez et al. [20].

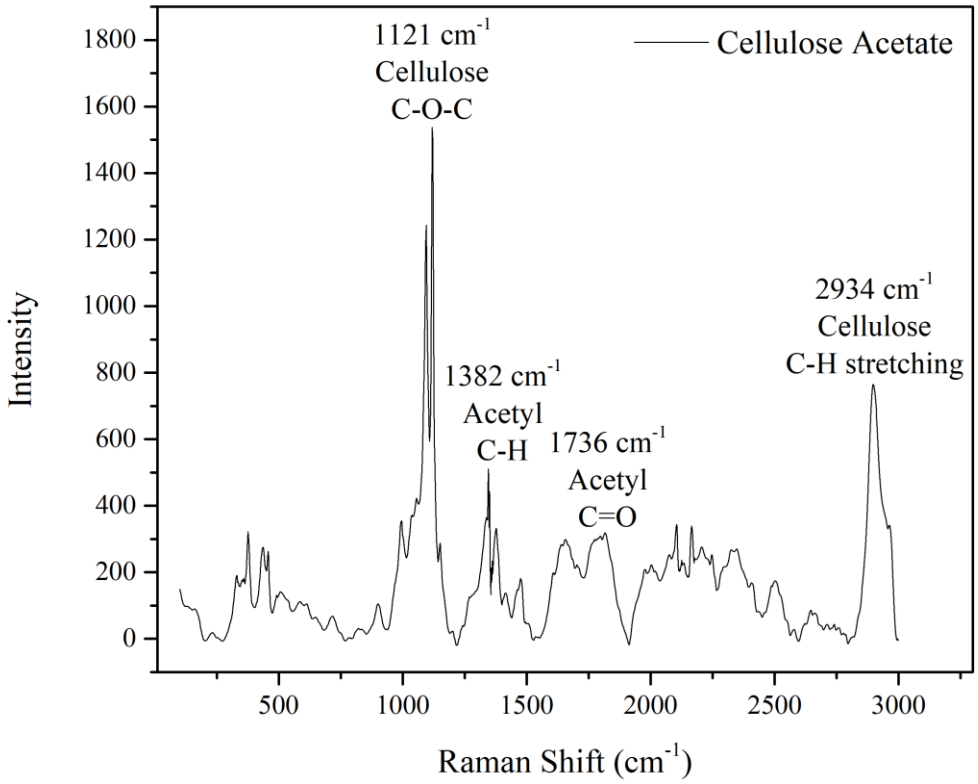

Figure 1: Raman spectrum of CA extracted from OPF

Characterization of TiO_2 and N-TiO_2

The synthesized TiO_2 and N-TiO_2 were characterized with Raman spectroscopy using green laser (514 nm) and FESEM using secondary electron (SE) detector. Figure 2 shows the Raman spectra of pure TiO_2 and N-TiO_2. The Raman spectra confirm the crystal phase of TiO_2 and N-TiO_2 which are of anatase-rutile mixture and pure anatase, respectively. The peak positions are compared with the Raman active fundamentals for anatase and rutile as reported by Ohsaka et al. [21]. For N-TiO_2 sample, the peaks at 144 cm^{-1}, 397 cm^{-1}, 514 cm^{-1}, and 636 cm^{-1} are attributed to E_g, B_{1g}, A_{1g} (superimposed with B_{1g}), and E_g modes of anatase phase, respectively. Whereas for pure TiO_2, the Raman shift at 435 cm^{-1} and 624 cm^{-1} are associated with E_g and A_{1g} modes of rutile, respectively. A_{1g}, B_{1g} and E_g modes are corresponding to the vibration of pure O, pure Ti and vibration mix of O-atom and Ti-atom motions, respectively [17]. Besides, the Raman active fundamentals suggested the addition of nitrogen to TiO_2 suppress the formation of rutile and induce the formation of pure anatase phase [14,22]. Anatase crystallinity may imply that the photocatalytic degradation of targeted pollutants using CA/N-TiO_2 membrane will be higher than CA/TiO_2 membrane since anatase phase is said to be more photoactive than rutile [19].

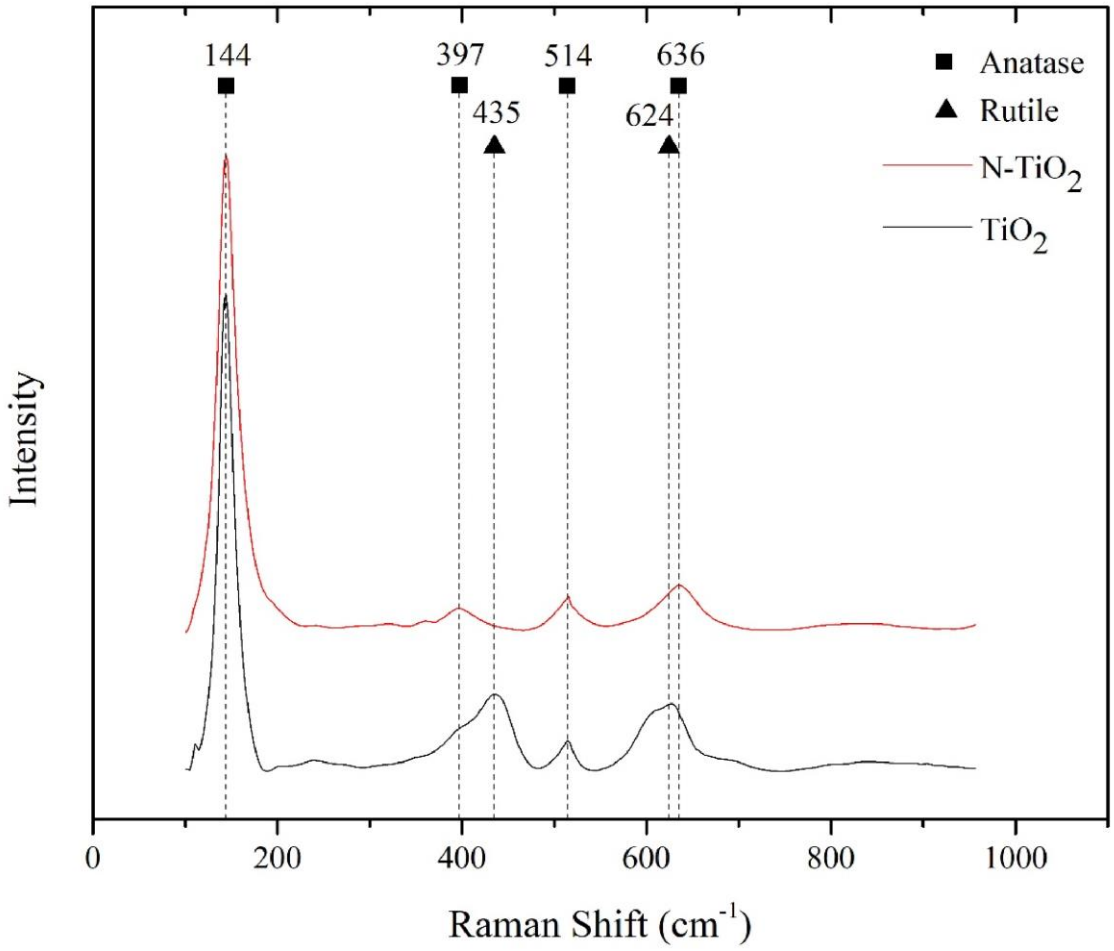

Figure 2: Raman spectra of TiO_2 and N-TiO_2

FESEM images of TiO_2 and N-TiO_2 samples in Figure 3 portray the surface morphology of the nanoparticles. Both samples show irregular shape and non-uniform sizes. The particles for TiO_2 samples are well-dispersed while the particles for N-TiO_2 are aggregated into larger clumps. Thus, TiO_2 has more active surface area compared to N-TiO_2 because the active sites are blocked due to aggregation. This is due to the thermal treatment done where N-TiO_2 sample was calcined up to 300°C while no calcination was done to pure TiO_2 samples. With increase of temperature, aggregation rate will increase as reported by Sathish et al. [13]. Average particle size for TiO_2 and N-TiO_2 are less than 20 nm. This corresponds with previous report where the average TiO_2 nanoparticles dimension and morphology are not significantly influenced by the addition of nitrogen [23].

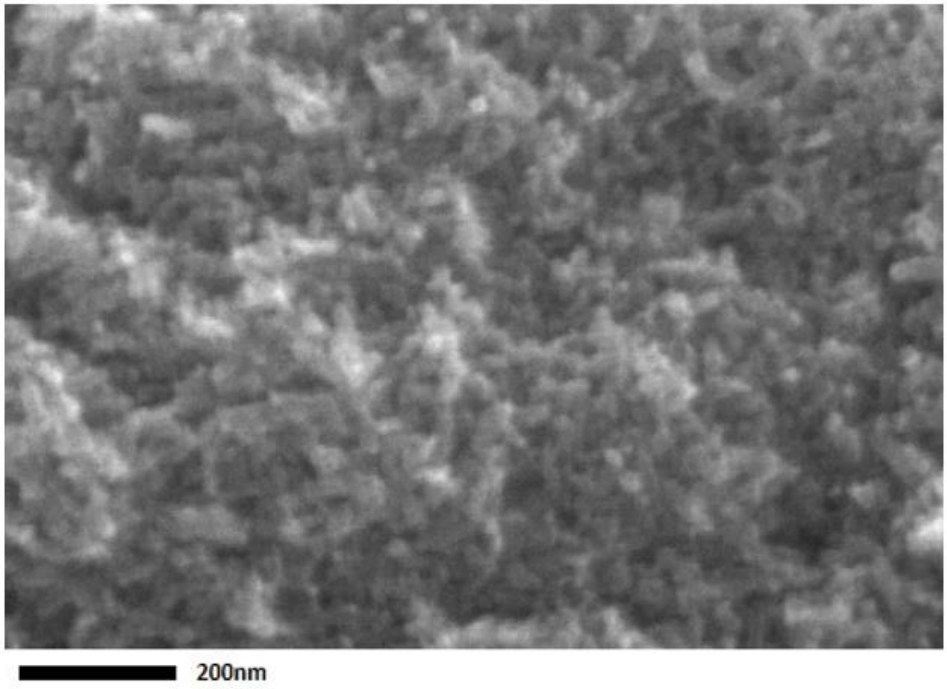

(a)

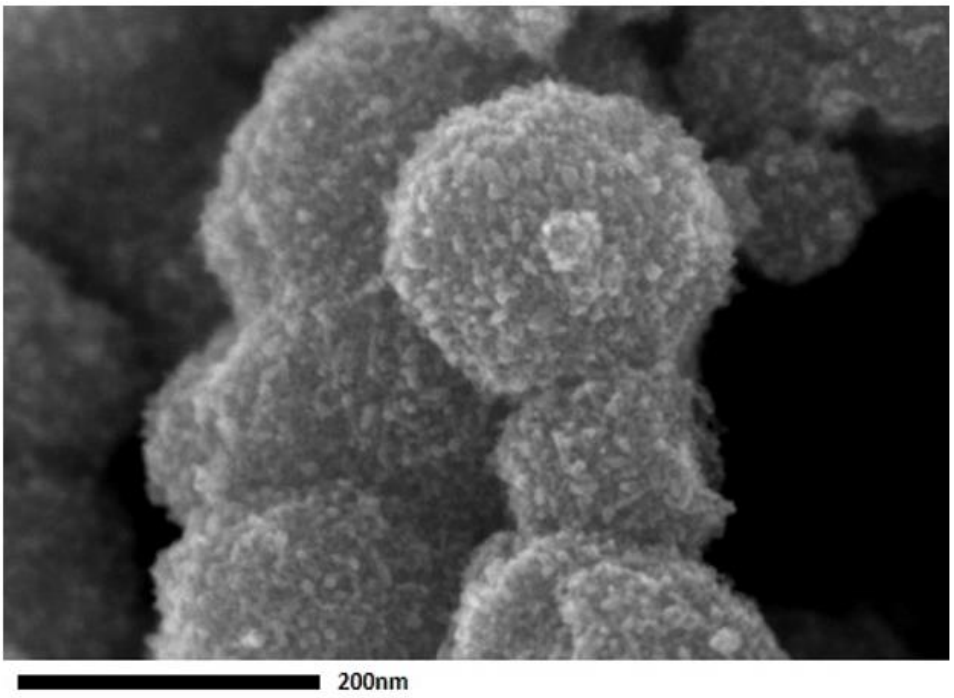

(b)

Figure 3: FESEM images of (a) TiO_2 at 100,000 × magnification; (b) N-TiO_2 at 200,000 × magnification

Characterization of Nano-PFTF membrane

Raman spectra of Nano-PFTF membrane shown in Figure 4 reveal the composition of the sample through the Raman peak positions. The fundamental Raman peaks for cellulose can be seen at 2939 cm^{-1} and 1128 cm^{-1} representing C-H stretching and asymmetric stretching vibration of the C-O-C glycosidic linkage. The fundamental Raman peaks for acetyl group are 1744 cm^{-1}, 1433 cm^{-1} and 1378 cm^{-1} which represents vibration of carbonyl C=O group, asymmetric vibration of C-H and symmetric vibration of C-H, respectively. The peaks at 1080 cm^{-1}, 978 cm^{-1}, 910 cm^{-1}, 839 cm^{-1}, and 656 cm^{-1} are referring to pyranose ring, C-O bond, C-H bond, O-H bond, and C-OH bond, respectively. The Raman spectra also confirm the presence of TiO_2 in the membrane, implying successful immobilization of titania particles within the membrane fiber matrix. The peaks at 144 cm^{-1} and 514 cm^{-1} are corresponding to anatase signals while 435 cm^{-1} for rutile. The Raman peak positions for TiO_2 also show that the titania embedded follows the individual TiO_2 and N-TiO_2 crystal phase which are anatase-rutile and anatase, respectively.

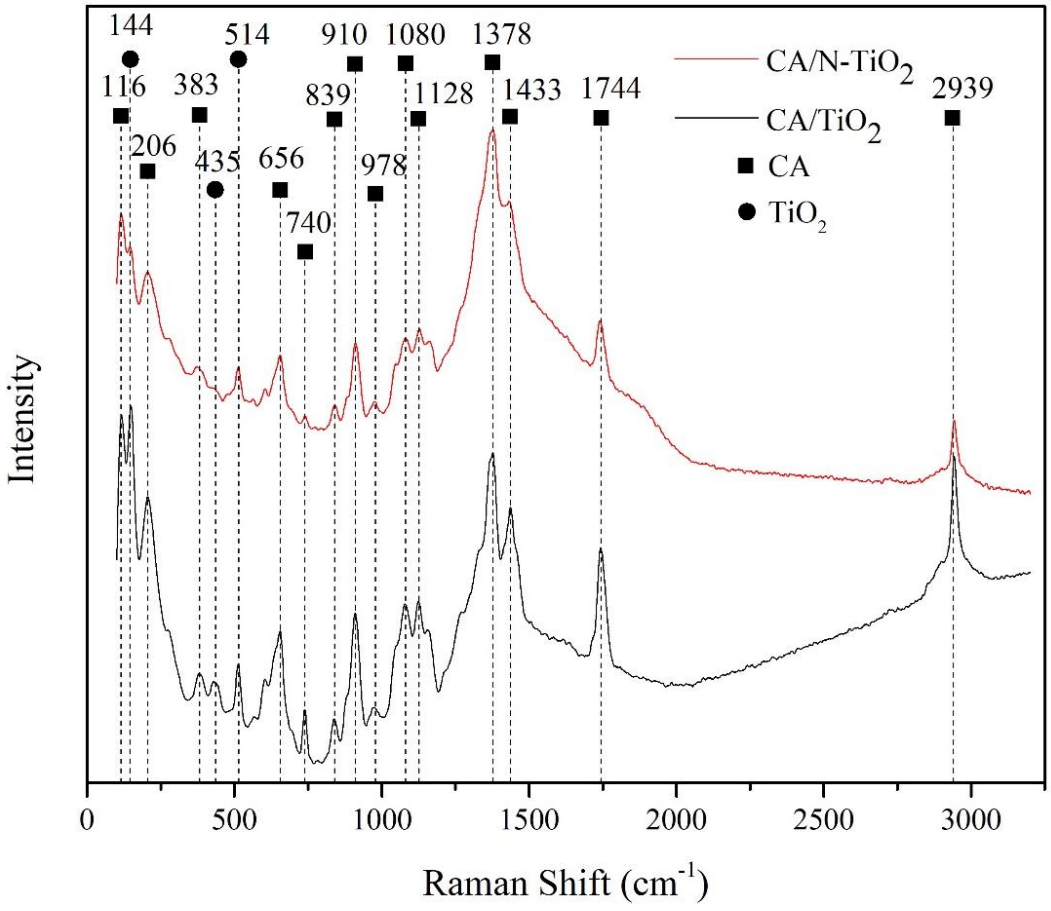

Figure 4: Raman spectra of Nano-PFTF membranes

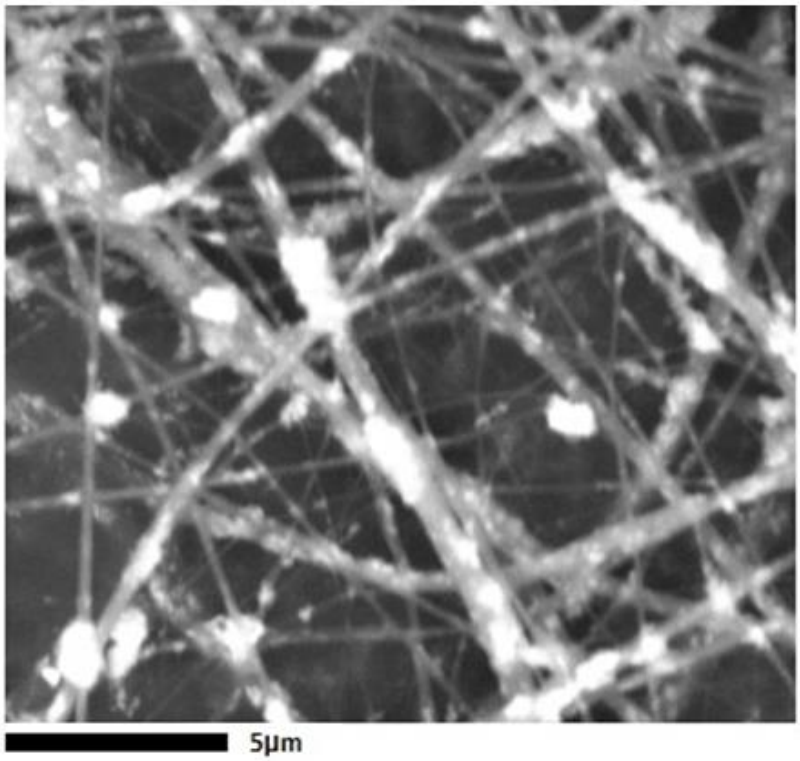

(a)

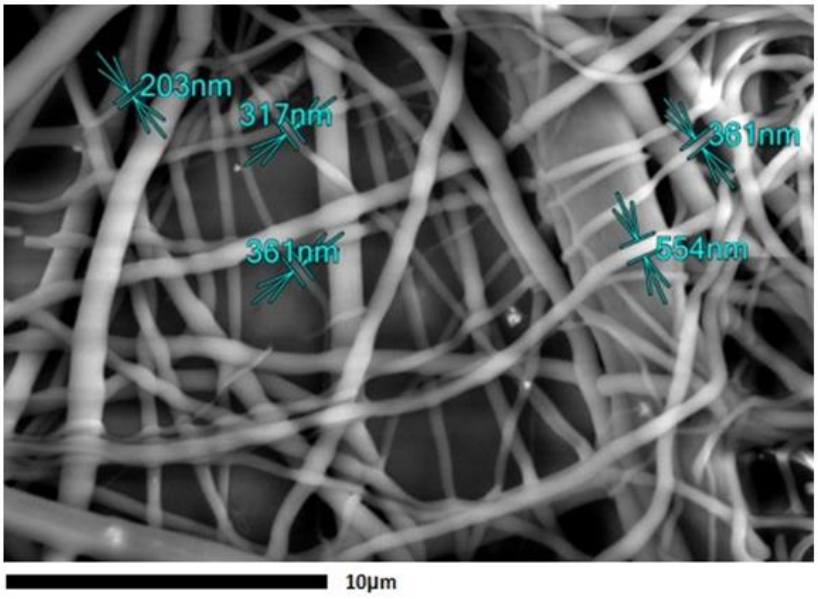

(b)

Figure 5: Surface morphology of Nano-PFTF membrane at (a) SEM 15,000 × magnification; (b) FESEM 5,000 × magnification

Upon immobilization of titania in the CA polymer solution to form the membrane, the

dispersion of titania in the membrane matrix is observed using SEM. The SEM images of CA/TiO_2 membrane at different magnifications are as shown in Figure 5a. The white spots are referring to TiO_2 particles embedded. It can be observed that TiO_2 particles are dispersed throughout the matrix. The weight loading of 2 wt% TiO_2 is considered optimum to produce nanofibers with visible titania beads and diameter between 222 – 346 nm [24]. In this study, the diameter of CA/N-TiO_2 membrane observed using FESEM ranging from 200 nm up to 500 nm as shown in Figure 5b.

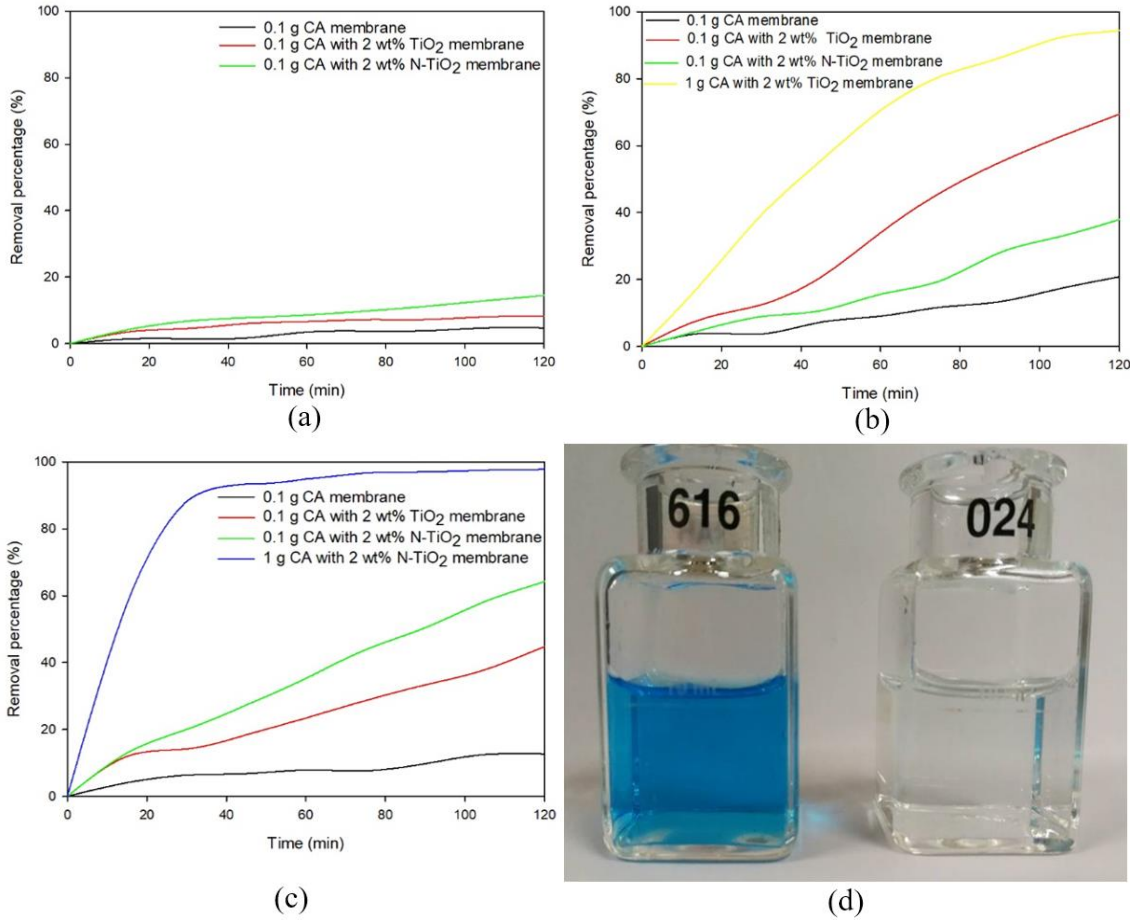

Figure 6: Removal percentage of MB for (a) control (b) UV light (c) visible light versus time (d) treated MB by 1 g CA with 2 wt. % N-TiO_2 membrane under visible light

Photocatalytic reduction of MB dye

Figure 6 shows the percentage of MB removal by CA membrane, CA with 2 wt.% TiO_2 membrane and CA with 2 wt.% N-TiO_2 membrane (i.e. Nano-PFTF membrane) under different light sources. As seen from Figure 6(a), there is only 4.68-14.45% removal after 2 h of stirring. The highest MB dye removal is achieved by CA membrane with 2 wt.% N-TiO_2, followed by 2 wt.% TiO_2, and lastly pure CA membrane. This can be explained by the surface morphology of the modified membrane as shown in Figure 5. The rougher and more porous surface of the modified membrane provides more active

sites for adsorption of dye molecules on the membrane surfaces. Besides, another factor contributing towards improved adsorption of MB dye is the increased negative charge of the membrane due to the incorporation of TiO_2 and N-TiO_2, [25]. Since MB dye is cationic in solution form, the opposite charge between the dye and TiO_2 could enhance the attraction between membrane and MB particles, hence improving adsorption [26].

For UV light degradation using 0.1 g of the membrane, the highest MB dye removal was achieved by a modified membrane with 2 wt.% TiO_2 (69.43%), followed by 2 wt.% N-TiO_2 (37.90%), then pure CA membrane (20.79%). This is inferred to be due to UV light excitation onto the TiO_2 particles. The study also in accordance to study conducted to degrade dye using nanocomposite *Nafion* membrane embedded with TiO_2 [27]. Their studies suggested that the degradation of dye follows the following reactions, excited dye molecules are generated upon absorption of visible photons, and subsequently inject electrons intro TiO_2. Consequently, dye molecules degrade in the wastewater.

On the other hand, for visible light degradation using 0.1 g of the membrane, the highest MB dye removal was achieved by a modified membrane with 2 wt. % N-TiO_2 (64.24%), followed by 2 wt. % TiO_2 (44.83%), then pure CA membrane (12.71%). As expected, a modified membrane with N-TiO_2 exhibited the higher visible-light photocatalytic activity dye to the effect of nitrogen doping into the TiO_2 lattice. This can be explained by the fact that, when the dopants were added, the N atoms replaced the oxygen sites of TiO_2. This increased the oxygen vacancy and Ti^{3+}, which leading an enhancement of photocatalytic activity [28]. Besides, the high activity of the N-TiO_2 may be ascribed to the reduction in particle size hence more active sites for dye adsorption [29].

By using the optimized membrane, 1 g of modified membranes with 2 wt. % TiO_2 and 2 wt. % N-TiO_2 was tested for both UV light and visible light source, respectively. As seen from Figure 6(b) and Figure 6(c), the MB dye removal is higher in visible light by a modified membrane with 2 wt. % N-TiO_2 (97.82%) than that of UV light using 2 wt. % TiO_2 membrane (94.40%). This could be due to higher porosity and adsorption surface area by N-TiO_2. A similar observation was also witnessed in the control experiment (Figure 6(a).

Photocatalytic reduction of Cr (VI)

Figure 7 shows the removal of 10 ppm Cr (VI) by modified membrane with 1 g of 2 wt.% TiO_2 (Nano-PFTF membrane) under UV light source. It is observed that the degradation process increased rapidly in the first 30 minutes and reaches stagnant towards the end of 2 h reaction time. The highest reduction of Cr (VI) was achieved at 99%. The Cr (VI) concentration after 2 h had dropped from 10 ppm to 0.1 ppm which has met the maximum concentration of Cr (VI) allowed in drinking water stipulated in WHO guidelines [30]. Generally, the Cr (VI) reduction rate by the photocatalytic-induced elections was significantly higher for acidic solution, in this case, pH 2-3 [31]. This is because TiO_2 surface carries more positive charges in acidic solution, the negatively-charged Cr (VI) species have a higher affinity towards the TiO_2, and thus

increase the extent of adsorption and photocatalytic reaction. The products of photocatalytic removal of Cr (VI) might be Cr (III) under acid pH [32].

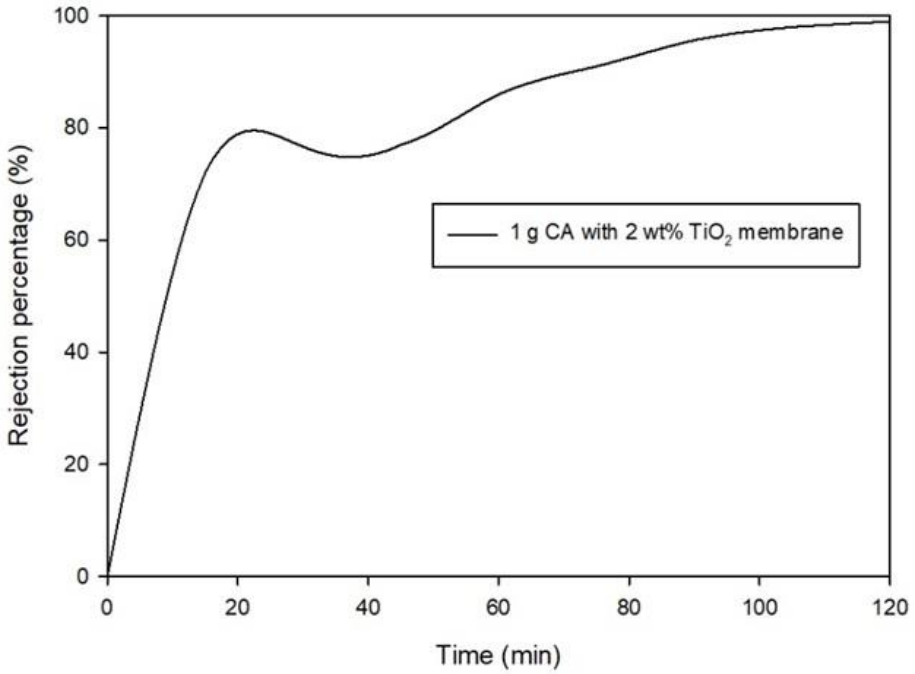

Figure 7: Rejection percentage of Cr (VI) by TiO_2 membrane under UV light versus time

Comparison of photocatalytic performance

The photocatalytic removal of MB dye and Cr (VI) with TiO_2 and N-TiO_2 was compared with other reports in the viewpoint of catalyst dosage, lamp power, reaction time, and removal efficiency as shown in Table 2 and Table 3, respectively. This comparison shows that the both TiO_2 and N-TiO_2 is an effective catalyst for the reduction of MB dye and Cr (VI) from aqueous solution. Based on the degradation results of MB and Cr (VI), the performance of fabricated Nano-PFTF membranes can be regarded as excellent. Thus, this product has a bright future as an efficient water treatment system to remove organic and inorganic pollutants in wastewater.

Table 2: Comparison of photocatalytic MB dye reduction results

System	Catalyst	Lamp	Time	Removal	Reference
UV/titanate nanotubes	0.5	8	120	90	[32]
Visible light/TiO_2 -	0.6	23	120	85.45	[33]
UV/TiO_2	0.4*	95	120	94.40	Present
Visible light/N-TiO_2	0.4*	125	120	97.82	Present

Table 3: Comparison of photocatalytic Cr (VI) reduction results

System	Catalyst	Lamp	Time	Removal	Reference
UV/titanate nanotubes	1	15	120	80	[31]
Visible light/TiO_2 -	1	125	120	78	[32]
UV/TiO_2	0.4*	95	120	99	Present
Visible light/N-TiO_2	0.4*	125	120	100	Present

*20 g/L membrane was used

CONCLUSION

The ability of Nano-PFTF membrane in removing the target contaminant indicates a successful merge between organic polymers with inorganic visible light active photocatalyst in producing a high-performance nanofiber membrane for water treatment. Nano-PFTF Membrane helps to enhance the wastewater treatment process by: (i) separating the pollutants from water through the membrane, and (ii) reduce the pollutants simultaneously with the presence of N-TiO_2 photocatalyst. Synthesized Nano-PFTF Membrane using CA-OPF and N-TiO_2 showed prominent removal percentage of MB dye and Cr (VI) of 97.82 % and 100 % respectively within 120 minutes of treatment using visible light lamp. Utilizing OPF for CA synthesis allows us to convert the largest portion of palm oil biomass into a nanomaterial of economic value which can be exploited for water treatment process. Overall, the production of Nano-PFTF membrane helps in environmental remediation by removal of dye and Cr (VI) on wastewater, and impacts the society by providing cleaner water, as well as enhances the value of OPF, a crop waste, to transform it into a potential nanomaterial. Further study on the characteristics of Nano-PFTF membrane should be done to improve its physico-chemical properties, as well as identifying wider range of pollutants that can be treated with this system.

ACKNOWLEDGEMENT

This work is made possible with the support from the NNC, MOSTI and strategic collaboration with technical partners from laboratories of Universiti Malaya, Universiti Kebangsaan Malaysia, Universiti Tun Hussein Onn Malaysia, Monash University Malaysia, Institut Teknologi Maju (ITMA) Universiti Putra Malaysia, Crest Analytics Sdn Bhd, Progene Link Sdn Bhd and Hi-Tech Instruments Sdn Bhd.

REFERENCES

[1] I.R. Hardin, in: Environ. Asp. Text. Dye., Woodhead Publishing Limited, 191–211 (2007)
[2] R. Kant, *Nat. Sci.* **4** 22–26 (2012)
[3] S.H.S. Chan, T.Y. Wu, J.C. Juan, C.Y. Teh, *J. Chem. Technol. Biotechnol.* **86**

1130–1158 (2011)
[4] A.M.L. Marechal, B. Križanec, S. Vajnhand, J. Volmajer, in: Org. Pollut. Ten Years After Stock. Conv. - Environ. Anal. Updat., 2012, pp. 29–56.
[5] M. Salem, Hanaa, A. Eweida, Eweida, A. Farag, *ICHEM 2000* 542–556 (2000)
[6] P.B. Tchounwou, C.G. Yedjou, A.K. Patlolla, D.J. Sutton, Molecular, *Clinical and Environmental Toxicology* **3** 133–364 (2014)
[7] A.A.I. Luthfi, S.F.A. Manaf, R.M. Illias, S. Harun, A.W. Mohammad, J.M. Jahim, *Appl. Microbiol. Biotechnol.* **101** 3055–3075 (2017)
[8] J.P. Tan, J.M. Jahim, S. Harun, T.Y. Wu, T. Mumtaz, *Int. J. Hydrogen Energy* **41** 4896–4906 (2016)
[9] C. Schütz, J. Sort, Z. Bacsik, V. Oliynyk, E. Pellicer, A. Fall, L. Wågberg, L. Berglund, L. Bergström, G. Salazar-Alvarez, PLoS One 7 (2012) 1–8.
[10] S.R.A.M. Rasli, I. Ahmad, A.M. Lazim, A. Hamzah, *Malaysian J. Anal. Sci.* **21** 1065–1073 (2017)
[11] Q. Wu, J. Zhao, G. Qin, C. Wang, X. Tong, S. Xue, *Appl. Catal. B Environ.* **142–143** 142–148 (2013)
[12] S.A. Ansari, M. Khan, O. Ansari, *New J. Chem.* **40** 3000–3009 (2016)
[13] M. Sathish, B. Viswanathan, *Korean Journal of Chemical Engineering* **22** (3) 358-363 (2005)
[14] B.M. Al-shabander, A. Ajaj, *Ekram, Eng. Tech. J.* **33** 1591–1598 (2015)
[15] M. Pelaez, N.T. Nolan, S.C. Pillai, M.K. Seery, P. Falaras, A.G. Kontos, P.S.M. Dunlop, J.W.J. Hamilton, J.A. Byrne, K. O'Shea, M.H. Entezari, D.D. Dionysiou, *Appl. Catal. B Environ.* **125** 331–349 (2012)
[16] Y. Nosaka, A. Nosaka, Introduction to Photocatalysis - From Basic Science to Applications, Royal Society of Chemistry, (2016).
[17] R.A. Zayadi, F.A. Bakar, *J. Photochem. Photobiol. A Chem.* **346** 338–350 (2017)
[18] R.G. Candido, A.R. Gonçalves, *Carbohydr. Polym.* **152** 679–686 (2016)
[19] T.P. Dhanya, S. Sugunan, *IOSR Journal of Applied Chemistry* **4** (3) 27–33 (2013)
[20] J.A. Sánchez-Márquez, R. Fuentes-Ramírez, I. Cano-Rodríguez, Z. Gamiño-Arroyo, E. Rubio-Rosas, J.M. Kenny, N. Rescignano, *Int. J. Polym. Sci.* **2015** (2015) https://doi.org/10.1155/2015/320631
[21] T. Ohsaka, F. Izumi, Y. Fujiki, *J. Raman Spectrosc.* **7** 321–324 (1978)
[22] M. Sathish, B. Viswanathan, R.P. Viswanath, C.S. Gopinath, *Chem. Mater.* **17** 6349–6353 (2005)
[23] V. Caratto, L. Setti, S. Campodonico, M.M. Carnasciali, R. Botter, M. Ferretti, *J. Sol-Gel Sci. Technol.* **63** 16–22 (2012)
[24] J. Geltmeyer, H. Teixido, M. Meire, T. Van Acker, K. Deventer, F. Vanhaecke, S. Van Hulle, K. De Buysser, K. De Clerck, *Sep. Purif. Technol.* **179** 533–541 (2017)
[25] Y.H. Teow, A.L. Ahmad, J.K. Lim, B.S. Ooi, *Desalination* **295** 61–69 (2012)
[26] M.N. Subramaniam, P.S. Goh, N. Abdullah, W.J. Lau, B.C. Ng, A.F. Ismail, *J. Nanoparticle Res.* **19** (6) 1-13 (2017)
[27] S. Filice, D. D'Angelo, S. Libertino, I. Nicotera, V. Kosma, V. Privitera, S.

Scalese, *Carbon N. Y.* **82** 489–499 (2015)
[28] X. Cheng, X. Yu, Z. Xing, L. Yang, *Arab. J. Chem.* **9** S1706–S1711 (2016)
[29] B.M. Rajbongshi, A. Ramchiary, S.K. Samdarshi, *Mater. Lett.* **134** 111–114 (2014)
[30] L.K. Bankole, S.A. Rezan, N.M. Sharif, *IOP Conf. Ser. Earth Environ. Sci.* **19** 012004 (2014)
[31] Y. Ku, I.L. Jung, *Water Res.* **35** 135–142 (2001)
[32] M.S. Siboni, M.T. Samadi, J.K. Yang, S.M. Lee, *Environ. Technol.* **32** 1573–1579 (2011)
[33] M.R. Delsouz Khaki, M.S. Shafeeyan, A.A.A. Raman, W.M.A.W. Daud, *J. Mol. Liq.* **258** 354–365 (2018)